

Optical fiber-based key for remote authentication of users and optical fiber line

Mikhail Yarovikov^{1,*}, Alexander Smirnov¹, Ekaterina Zhdanova¹, Alexander Gutor¹, and Mikhail Vyatkin¹

¹Terra Quantum AG, Kornhausstrasse 25, CH-9000 St. Gallen, Switzerland

*mj@terraquantum.swiss

ABSTRACT

We have shown the opportunity to use the unique inhomogeneities of the internal structure of an optical fiber waveguide for remote authentication of users or an optic fiber line. Optical Time Domain Reflectometry (OTDR) is demonstrated to be applicable to observing unclonable backscattered signal patterns at distances of tens of kilometers. The physical nature of the detected patterns was explained, and their characteristic spatial periods were investigated. The patterns are due to the refractive index fluctuations of a standard telecommunication fiber. We have experimentally verified that the patterns are an example of a Physically Unclonable Function (PUF). The uniqueness and reproducibility of the patterns have been demonstrated and an authentication protocol has been provided.

Introduction

Fiber-optic lines are a common way to transmit information¹. An authentication is a practical approach to ensuring that data is transferred to a proper recipient².

An option for authentication is the use of Physically Unclonable Functions (PUFs)³. They are objects with a unique non-reproducible structure which brings particular responses on different physical exposure. Researches have studied vast variety of PUFs of different physical nature⁴. A significant part is optical PUFs, where the interference plays the main role. Such PUFs may use biological layers⁵, chemical solutions⁶, irregular 2D-surfaces⁷ as optical tokens. Some of them utilize optical fibers as scattering media⁸ or a waveguide⁹. The presence of the interference strictly limits the remote authentication properties of the conventional optical PUFs.

Additionally, an experimental approach for identifying fiber sections based on Rayleigh scattering¹⁰ analysis has been proposed^{11,12,13,14}. This approach is based on Optical Frequency Domain Reflectometry (OFDR)¹⁵. OFDR is characterized by a very high spatial resolution down to fractions of a millimeter. On the other hand, it has distance limitations: it does not allow to look further than one-two kilometers, which is a severe disadvantage to remote measurements. In addition, the characteristic spatial periods of the observed backscattered light patterns have not been studied so far.

In this paper, we provided the physical model describing the mechanisms of these patterns occurrence and demonstrated that patterns can be processed via Optical Time Domain Reflectometry (OTDR). Although conventional OTDR devices have worse spatial resolution than OFDR, they allow measurements over significantly longer distances and are limited only by attenuation in the waveguide. Therefore, the more extensive distance range of OTDR devices is an essential advantage for remote authentication. We considered the optical fiber sections in terms of PUF and interpreted OTDR-processed patterns obtained at distances of tens of kilometers as a "reflectokey" – the unique signal that can be used for authentication. We experimentally checked the uniqueness and reproducibility of these patterns and suggested an authentication protocol. We investigated the spatial spectrum of OTDR-processed patterns and experimentally showed that they have a wide range of spatial frequencies, and could be detected at various spatial scales.

Method description

The optical fiber span is a unique physical object itself. A preform for the fiber core is made of silica and doped with, e.g., Al, P, N, Ge, for fiber to have waveguide properties. Silica is an amorphous substance and every piece of it has a unique structure at the atomic level. Dopant atoms are randomly incorporated into the silica structure. All of the internal structure features are less than wavelength λ , and the light experiences Rayleigh scattering¹⁰. The physical uniqueness of the optical fiber can also be observed on much larger spatial scales, since it is also due to the specifics of the manufacturing of optical fiber. And it can be detected via reflectometry methods such as OFDR and OTDR. This uniqueness provides the opportunity to obtain distinctive backscattered signal, a "reflectokey", which will authenticate any specific section of the fiber line.

OTDR device sends the light pulses of specific wavelength, shapes and durations to probe the optical fiber line¹⁶. Each of the pulses generates a backscattered signal that characterizes the line. A reflectogram is the logarithmic dependence of the backscattered radiation intensity on the distance. Mathematically, a reflectogram is a convolution of a probing pulse and a particular function implying the unique individual extended characteristics of the optical fiber. In the next section, we provide a theoretical justification for this fact and prove that the reflectogram of the fiber line can be used to obtain authentication data, since it implicitly contains information about the physical uniqueness of the fiber.

For homogeneous optical fibers, a linear decrease in the level of backscattered radiation, expressed in dB, with distance along the fiber is expected. However, in practice, it is easy to see that deviations from the linear decay take place (see an example in Figure 1).

These fluctuations consist of two contributions. The first one is due to random noises. These include the noise of the reflectometer components, e.g., laser source or photodetector. Actually the contribution of noises can be almost entirely eliminated by a proper averaging or using of a more accurate equipment. The second contribution is due directly to the unique inhomogeneities of the optical fiber.

First of all, these are refractive index inhomogeneities, which are both local and non-local due to the technological features of fiber preform manufacturing. Moreover, additional technical inhomogeneities appear when manufacturing the optical fiber, associated with the variability of the fiber geometry. Although special equipment controls the constancy of the core diameter when drawing the fiber from the preform, control accuracy exceeding a fraction of a percent is not a goal. In turn, even a tiny change in the core diameter may lead to a change in the resulting backscattering factor, which entails a difference in the level of the backscattered signal. All these effects contribute to the observed fluctuations in the reflectogram. This contribution determines the variations in the reflectogram shown in Figure 1. And it is this contribution that we propose to use as a unique key for the corresponding fiber section, its "fingerprint".

These unique patterns can be observed, e.g., by subtracting the linear contribution from the reflectogram. Figure 2a shows an example of the processing result for a 1 km section of standard SMF-28e (ITU-T G.652.D) single-mode telecommunication fiber. The measurements were carried out with a standard OTDR device at a wavelength of $\lambda=1550$ nm with a pulse duration of 500 ns and averaging over 2^{10} experiments, which is enough for the elimination of random noises.

It can be experimentally verified that in successive measurements with the same pulse parameters, the patterns for the same fiber section are reproduced with high accuracy (see Fig. 2b). As a mathematical metric for evaluating the accuracy of patterns reproducibility, the value of the correlation coefficient for experimental data arrays is considered. In this approach, high accuracy of patterns reproducibility corresponds to correlation coefficient value close to +1, while value in the vicinity of 0 indicates a lack of reproducibility. Joint correlation matrices corresponding to the series of successive measurements were analyzed.

Results

Theoretical analysis

The source of the observed patterns is the variations of backscattered Rayleigh radiation. It is of interest how the backscattered light implies information about the internal properties of fibrous media. The signal is formed by local scattering acts, which are determined by local properties of the fiber: refractive index, attenuation constant and backscattering factor, which may vary with distance. These values variations over fiber length should be described and connected with detected power. Following the standard approach^{17,18} we derive these variations.

To obtain the backscattered power from a local fiber section, let us consider initial linearly polarized speculative electrical pulse propagating in the fiber in z direction as

$$E(x, y, z_p, t) = E_0 \hat{\psi}(x, y) f(v_{gr}t - z_p) \cos \beta (v_{ph}t - z_p) \exp\left(-\frac{1}{2} \int_0^{z_p} \alpha(\xi, \beta) d\xi\right), \quad (1)$$

where $f(v_{gr}t - z_p)$ denotes the rectangular unit envelope function with length l , $\hat{\psi}(x, y)$ – field distribution of the fundamental mode, β – propagation constant, α – attenuation constant which depends on coordinate and $v_{ph,gr}$ – phase and group speeds of light, correspondingly.

The differential amplitude (at the moment t in $z = 0$) of the electric field scattered from section dz at the point $z = z_s$:

$$dE_s(x, y, z_s, t) = dz_s \frac{E_0}{\pi w_0^2 n c} \hat{\psi}(x, y) \exp(-z_s \bar{\alpha}(z_s)) \sin \beta (v_{ph}t - 2z_s) f(v_{gr}t - 2z_s) \times \left(\int_S dx dy \Delta \chi(x, y, z_s) |\hat{\psi}|^2(x, y) \right), \quad (2)$$

where $\Delta \chi(x, y, z_s)$ denotes the local inhomogeneities of electrical susceptibility which cause the scattering, $\bar{\alpha}(z_s)$ denotes averaged value of $\alpha(z)$ over the distance $[0; z_s]$, w_0 denotes the mode field diameter while the field distribution is assumed

to have a Gaussian form: $\hat{\psi}(x, y) = \exp(-(x^2 + y^2)/w_0^2)$. Mode field distribution, in general, may slightly vary on z , but this dependence is insignificant since these fluctuations are averaged.

Integration over the pulse length gives the following:

$$E_s(x, y, t) = \int_{v_{gr}t/2-l/4}^{v_{gr}t/2+l/4} dE_s(x, y, z_s, t). \quad (3)$$

Now we assume that the exponential decay $\exp(-z_s \bar{\alpha}(z_s))$ does not change on the scales of the wavelength. That is true for the typical attenuation constant α which is about $0.18 - 0.24$ dB/km. Moreover, this is also justified by the fact that α makes sense only on the scales of several wavelengths. This makes it possible to average by time period and calculate the backscattered power:

$$P_s(t) = \int_S dx dy \langle E_s^2 \rangle_T / \sqrt{\mu/\epsilon} = P_0 \left(\frac{\omega}{c} \right)^2 e^{-\bar{\alpha} v_{gr} t} \frac{Q(t)}{n^2 (\pi w_0^2)^2}, \quad (4)$$

where the initial power is $P_0 = (1/2) (E_0^2 / \sqrt{\mu/\epsilon}) (\pi w_0^2 / 2)$ and

$$Q(t) = \left| \int_{v_{gr}t/2-l/4}^{v_{gr}t/2+l/4} dz_s e^{2i\beta z_s} \int_S dx dy \Delta \chi(x, y, z_s) |\hat{\psi}|^2(x, y) \right|^2. \quad (5)$$

For further simplicity, we denote the probing pulse center coordinate by $z = v_{gr}t/2$. The backscattered power at the input of the fiber at the moment t corresponds to backscattering from the section of $l/2$ length at the point z . We suppose l at least several times larger than both atomic scales and wavelength:

$$Q(z) = |\hat{\chi}_{2\beta}(z)|^2 = \left| \int_{z-l/4}^{z+l/4} dz_s e^{2i\beta z_s} \bar{\Delta \chi}(z_s)_S \right|^2, \quad (6)$$

where $\bar{\Delta \chi}(z_s)_S$ denotes a weighted average of $\Delta \chi(x, y, z_s)$ with the squared distribution of the fundamental mode $|\hat{\psi}|^2(x, y)$. $Q(z)$ in (6) can be treated as the squared absolute value of spatial Fourier transform of magnetic susceptibility with spatial vector 2β of the fiber section in the vicinity of the point z . The equation (4) can be rewritten as:

$$P_s(z) = \frac{P_0}{n^2 (\pi w_0^2)^2} e^{-2z\bar{\alpha}} \left(\frac{\omega}{c} \right)^2 |\hat{\chi}_{2\beta}(z)|^2, \quad (7)$$

Equations (6) and (7) completely describe the scattering process in single-mode optical fibers, how the reflected light brings the information about internal structure of the fiber. The power scattered from the vicinity of the auxiliary point of the fiber is defined by the local magnetic susceptibility distribution, refraction coefficient and mode field distribution. The mode field distribution may also vary in different fiber sections due to geometry defects and refractive index variability. Following the results obtained in previous works^{17,18} $|\hat{\chi}_{2\beta}(z)|^2$ can be linked with observable value $\alpha(z)$:

$$\alpha(z) = \frac{4(\omega/c)^4}{3\pi^2 w_0^2(z) l} |\hat{\chi}_{2\beta}(z)|^2. \quad (8)$$

In equation (8) $\alpha(z)$ is the coefficient of loss due to the scattering. Similar to $|\hat{\chi}_{2\beta}(z)|^2$ in (6), α in (8) can be defined only at a fiber section the size of at least several wavelengths. Otherwise, it losses its physical meaning. Preferably, this fiber section length $l/2$ should be more than several dozens of wavelengths. Together with the backscattering factor, it determines the power scattered in the backward direction. Thus, from (8) we can see that apart from the refractive index and the mode field diameter, possible variations of the backscattered radiation are due to possible oscillations of $|\hat{\chi}_{2\beta}|^2$ along the fiber.

To derive the power of the real pulse backscattered from the length $l/2$, let us substitute (8) into (7) and obtain:

$$P_s(z) = P_0 \frac{l}{2} \alpha(z) B(z) e^{-2z\bar{\alpha}} = W \frac{v_{gr}}{2} \alpha(z) B(z) e^{-2z\bar{\alpha}}. \quad (9)$$

Here $B(z) = \frac{3}{2n(z)^2 w_0(z)^2} (\frac{c}{\omega})^2$ denotes the backscattering factor with $n(z)$ and $w_0(z)$ depending on distance in general case. $W = P_0 \tau = \frac{P_0 l}{v_{gr}}$ denotes a pulse energy.

$P_s(z)$ from (9) may be considered as backscattered power from a delta-like probing pulse. This assumption is justified for a narrow pulse. As discussed above, the pulse length should be not less than several wavelengths. This length should be more than the coherence length to avoid interference effects. In this consideration $\alpha(z)$ can be treated as value at the point.

W corresponding to delta-pulses should be replaced with $W \cdot F(v_{gr}t - 2z)dz$ for general case of extended pulses. Here a normalized power envelope function $F(z - v_{gr}t)$ describes the pulse shape. The backscattered power for extended pulses may be expressed as

$$P_s(t) = \frac{Wv_{gr}}{2} \int_0^L dz \alpha(z) B(z) F(v_{gr}t - 2z) e^{-2z\bar{\alpha}}. \quad (10)$$

Thus, the backscattered power is a convolution of the pulse with $\alpha(z)$ and $B(z)$, which describe the unique scattering properties of the optical fiber. E.g., for the rectangular optical pulses relatively short compared to an exponential decay (10) takes the form of a window averaged product of α and B :

$$P_s(t) = \frac{Wv_{gr}}{2} \overline{\alpha(z)B(z)}_{[z-\delta/4, z+\delta/4]} e^{-2z\bar{\alpha}}, \quad (11)$$

where δ corresponds to the pulse length. This equation demonstrates that individual scattering properties may be observed through conventional OTDR technology where the typical pulse duration is $\sim 1 \text{ ns} - 10 \mu\text{s}$ ($\sim 0.2 \text{ m} - 2 \text{ km}$).

Rayleigh scattering is due to fluctuations of $\Delta\chi(x, y, z_s)$ on the scales less than optical signal wavelength. These small-scale fluctuations, often regarded as white spatial noise, determine the value of $|\hat{\chi}_{2\beta}|^2$, which causes the optical signal backscattering. Otherwise, the inhomogeneities in optical fibers are in an extensive range of spatial scales. Therefore, they will define variations of $|\hat{\chi}_{2\beta}|^2$ on scales larger than the optical signal wavelength. As these $|\hat{\chi}_{2\beta}|^2$ variations in an optical fiber may have an extensive spatial range on the larger scales, they can also be described, at first approximation, as the white spatial noise. These large-scale variations can be observed with, e.g., conventional OTDR technique.

Experimental verification of fiber key uniqueness and reproducibility

As mentioned above, variations remaining on the reflectogram (i.e. patterns) are due to different chaotically distributed inhomogeneities of the fiber waveguide. And since it is technologically impossible to reproduce the exact locations of such inhomogeneities, the fiber sections can be considered in terms of PUF in the language of challenge-response pairs³. As a result, they, as physically unique objects, can be used as keys for authentication after conducting reflectometric measurements (in our case, OTDR measurements) with light pulses having predetermined parameters.

As was stated earlier, the OTDR technique may demonstrate several kinds of instability, particularly in laser pulse intensity or shape impermanence, photodetector noises, delay mismatching, etc. This instability may not be eliminated sufficiently by proper averaging to achieve the required properties of uniqueness and reproducibility. Thus, these properties should be clearly verified experimentally.

To confirm the uniqueness, the successive series of measurements were carried out with the same pulse parameters for two independent sections of the same fiber having the same length. Five consecutive measurements were made for each fiber section. Based on obtained patterns, the joint correlation matrix was constructed. This matrix is presented in Figure 3a. The patterns of fiber sections are individually well reproduced (red blocks), as the values of the standard correlation coefficient are not less than 0.93. On the other hand, patterns of independent sections of the fiber are entirely different (blue blocks), since the absolute values of the correlation coefficient do not exceed 0.26. One can see that even sections of the same fiber may be distinguished with a high degree of accuracy.

Reflected power is conjointly determined by probing pulse and fiber waveguide properties. Therefore, if the parameters of the pulse vary, the resulting patterns may also change. An increase in the duration of pulses leads to deterioration in the effective spatial resolution of the OTDR device, thereby eliminating the variations with high spatial frequencies and changing the appearance of patterns. Thus, the same fiber affected by pulses with distinct shapes should produce essentially different patterns. To experimentally confirm this fact, we measured a fixed section of the fiber, but with different pulse duration: 500 ns and 1000 ns. In Figure 3b a similar matrix is given. The patterns for each series of measurements individually are again well reproduced since the correlation coefficient values are at least 0.90. Still, when the pulse parameters change, the patterns become entirely independent.

The conducted experiments show that when performing OTDR measurements of an optical fiber section, the unique patterns are formed by both the fiber's internal structure and pulse. Thus the patterns change significantly when the fiber section or the pulse parameters are altered.

According to that, the evolution of correlation coefficient values over time was investigated. The measurements were carried out for the section of the same single-mode fiber 400 m long. Twenty five measurements were sequentially made on one day and the same number of measurements a week later. Figure 4 shows the corresponding joint correlation matrix. All

matrix elements are greater than 0.80, which indicates good reproducibility of patterns with time. It is also worth noting that an increase in the fiber section length leads to additional reproducibility improvement.

Obtained patterns demonstrate uniqueness and reproducibility, which are required for identification purposes. So that, experimental results prove that an optical fiber section may be recognized in the authentication procedure.

Spatial frequencies spectrum investigation

On the one hand, we experimentally observed unique patterns on the scales of tens of kilometers with the resolution from tens to hundreds of meters. On the other hand, patterns may also be observed with the OFDR technique on the scales of meters with submillimeter resolution^{11, 12, 13, 14}. These patterns correspond to independent variations of the fiber media. As unique patterns can be observed in a wide range of spatial scales, it is of interest to investigate the spatial spectrum.

To determine characteristic spatial frequencies of observed variations of patterns, the discrete Fourier transform (DFT) of patterns has been carried out (see Fig. 5a). For convenience, the spatial vector \mathbf{k} was used, related to the spatial period Λ as $k = \frac{2\pi}{\Lambda}$. The patterns were obtained in OTDR measurements of the 25 km long fiber line with pulse durations of 200 ns and 1000 ns (see Fig. 5b).

According to the results, the spatial spectrum is dense with frequencies from $\sim 10^{-4} \text{ m}^{-1}$ to $\sim 10^{-1} \text{ m}^{-1}$. Moreover, for both pulse durations, the amplitudes of the lowest spatial frequencies have essentially non-zero values (see the subplot in Fig. 5a). Thus spatial periods of variations of patterns may reach scales of the length of fiber line and are limited only by OTDR distance range or the fiber length. Moreover, on these scales, spatial frequencies have fairly close values for different pulse durations since the length of the fiber line is significantly greater than the pulse lengths.

In a high spatial frequency region, the spectrum is limited by the pulse length, which determines the spatial resolution of a device, in a lower frequency region – by the fiber length. As an estimate of the boundary for high spatial frequencies, we considered the point at which the Fourier transform value is halved compared to the maximum. For convenience, a polynomial approximation was applied to the data (see curved lines in Fig. 5a). For the selected pulses, these boundaries correspond to a spatial period of about fifty meters for a pulse duration of 200 ns and about two hundred meters for a pulse duration of 1000 ns. These values are of the order of corresponding pulse lengths in the fiber waveguide which are $l = c \cdot \tau_p$, where $c = 2 \cdot 10^8 \text{ m/s}$ denotes the speed of light in optical fiber, τ_p – the duration of the pulses.

The above results indicate that OTDR-processed patterns variations can be observed in a wide range of spatial periods – from tens of meters to tens of kilometers. Considering the results presented in OFDR experiments, the overall spectrum extends from submillimeter scales to tens of kilometers and possibly even greater values. Since the spectrum is so broad and dense, the patterns' oscillations' structure is similar to the white noise. Furthermore, the abovementioned observations provide extremely high robustness against altering the fiber section by the intruder. These results confirm the opportunity to use these patterns to authenticate remote users or fiber sections of various lengths.

Proposed application

Line authentication

The uniqueness of the patterns obtained from OTDR measurements can be used for the authentication of important sections of a fiber line or almost the entire line. As a possible authentication protocol, the following sequence of actions is suggested for the user of the fiber line:

1. User first carries out OTDR measurements with a large variety of available challenge pulses to form a challenge-response pairs database in digitized form.
2. To authenticate an optical line legitimate user needs to carry out OTDR measurements with randomly selected challenge pulse(s) from his database and collect response(s).
3. Then the user takes an appropriate mathematical comparison method (e.g., correlation metrics) for his response(s) and gets the result of whether the authentication is successful.

Since OTDR technology allows measurements without breaking the line integrity, the authentication process can be performed at any time convenient for the user. Authentication can be performed simultaneously with the transmission of information over the line. This approach requires Wavelength Division Multiplexing (WDM) technology or Optical Time Division Multiplexing (OTDM) approach.

Users authentication

The individual sample of fiber can be used to authenticate the particular legitimate user. If it is necessary to exchange information between two users, they will first connect their fiber samples, each from its side, and authenticate each other in turn. The physical connection can be implemented, e.g., by employing optical connectors or fusion splices.

The following authentication protocol is proposed on the example of a two-user model (Alice and Bob):

1. Both Alice and Bob, with their OTDR devices, carry out in advance numerous measurements of each other's unique fiber samples with a wide variety of probing pulse parameters, i.e., form two databases of challenge-response pairs³.
2. For Alice to authenticate Bob, he connects his unique fiber sample to the receptacle. Then, Alice randomly selects challenge-response pair(s) from her database and sends the light pulses with corresponding parameters to Bob.
3. In case of correct response in terms of the chosen method of mathematical comparison, Bob authenticates Alice the same way.
4. In case of correct responses from both sides, authentication is successful.

To improve the quality of authentication when working with long fiber lines, legitimate users can prepare their unique samples consisting of special fibers with an increased Rayleigh backscatter coefficient. This approach will increase the intensity of backscattered radiation and improve the recognition rate of patterns. In Figure 6 a conceptual scheme of the authentication of legitimate users and the entire line is given.

Possible actions of eavesdropper

During the authentication process, an interceptor could try to infiltrate the line, seeking to fake the backscattered radiation signal necessary for successful authentication to mislead the legitimate user. Nevertheless, the interceptor will not be able to falsify the signal. Since only the legitimate user knows the selected pulse parameters during measurements, the eavesdropper will not be able to reproduce the unique patterns of the fiber line section, as they vary depending on the probing pulse parameters. Moreover, the legitimate user can send trains of interleaved pulses with a complex structure and also control backscattered signals' arrival time. With this approach, the eavesdropper will not be able to accurately fake the patterns required for successful authentication because analyzing the parameters of the sent pulses and resending the fake signals interceptor will introduce a significant time delay, which the legitimate user will detect immediately. Upon receipt of unsatisfactory or doubtful results, the legitimate user has the right to consider the authentication failed.

Conclusion and discussion

We demonstrated a conventional OTDR technology as a convenient instrument for investigating unique variations of backscattered Rayleigh radiation in optical fiber waveguides. The patterns obtained from reflectograms of the fiber sections were detected in a wide range of spatial scales from tens of meters to tens of kilometers. The physical origin of the observed patterns is a convolution of optical pulse with a unique scattering profile of the fiber. The fiber manufacturing process explicitly implies the presence of extended inhomogeneities, which allow the observation of patterns on an even broader scale from submillimeter range to hundreds of kilometers. Observed spatial oscillations spectra are broad and dense in three orders of magnitude range.

The uniqueness and reproducibility of the patterns have been experimentally verified using standard correlation metrics. That fulfills the requirements for authentication procedure. As a result, the authentication procedures for the optical fiber line sections or legitimate remote users were proposed.

It is worth emphasizing that the considered variations of the backscattered signal level are in no way connected with interference effects, on which many optical PUFs are based⁴. The explanation of the interference absence is that the coherence length of the OTDR device laser source is smaller than the length of the probing pulses¹⁹, namely, $l_c \ll l_p$. These lengths can be estimated as $l_c \sim \frac{\lambda^2}{\Delta\lambda} \lesssim 10^{-4}$ m and $l_p \sim c \cdot \tau_p \gtrsim 10$ m, respectively, where $\Delta\lambda \sim 10^{-8}$ m – the width of the spectral range of pulses of the OTDR device used in our experiments, $c = 2 \cdot 10^8$ m/s – speed of light in optical fiber waveguide, $\tau_p \gtrsim 100$ ns – the duration of the used probing pulses. The absence of interference gives an advantage over conventional interference-based optical PUFs due to the patterns' stability in time and remote control availability. If interference effects were present, we would not be able to observe the reproducibility of patterns after a long time because of temperature and mechanical vibration effects. As the time between the measurements was significant, a difference in the ambient temperature and, as a result, in the fiber temperature inevitably occurred. And since the refraction coefficient of the optical fiber and fiber length significantly depend on temperature, the optical paths lengths also change with temperature. The alteration of the latter would essentially vary the interference results.

Future work in this area may study the effect of external physical conditions on the reproducibility of backscattering patterns. It is also of interest to involve more advanced mathematical methods in evaluating the uniqueness of patterns, particularly machine learning and neural network technologies. It is worth adding that the length of fiber lines suitable for applying the described approach is limited only by the attenuation of the fiber. Modern OTDR devices can handle lines with lengths on the order of hundreds of kilometers. Moreover, the OTDR distance range could be increased by installing bi-directional optical amplifiers in the line. This approach could be a perspective for further investigation.

Data availability

All materials that support the results of this study are available from the corresponding author on reasonable request.

References

1. Azadeh, M. Fiber optic communications: A review. *Fiber Opt. Eng.* 1–27, DOI: https://doi.org/10.1007/978-1-4419-0304-4_1 (2009).
2. Wu, B., Shastri, B. J. & Prucnal, P. R. Secure communication in fiber-optic networks. *Emerg. Trends ICT Secur.* 173–183, DOI: <https://doi.org/10.1016/B978-0-12-411474-6.00011-6> (2014).
3. Maes, R. & Verbauwhede, I. Physically unclonable functions: A study on the state of the art and future research directions. *Towards Hardware-Intrinsic Secur.* 3–37, DOI: https://doi.org/10.1007/978-3-642-14452-3_1 (2010).
4. McGrath, T., Bagei, I. E., Wang, Z. M., Roedig, U. & Young, R. J. A puf taxonomy. *Appl. Phys. Rev.* **6**, 011303, DOI: <https://doi.org/10.1063/1.5079407> (2019).
5. Wan, Y. *et al.* Bionic optical physical unclonable functions for authentication and encryption. *J. Mater. Chem. C* **9**, 13200–13208, DOI: <https://doi.org/10.1039/DITC02883A> (2021).
6. Arppe-Tabbara, R. & Sørensen, T. Physical unclonable functions generated through chemical methods for anti-counterfeiting. *Nat. Rev. Chem.* **1**, 0031, DOI: <https://doi.org/10.1038/s41570-017-0031> (2017).
7. Cao, Y. *et al.* Optical identification using imperfections in 2d materials. *2D Mater.* **4**, DOI: <https://doi.org/10.1088/2053-1583/aa8b4d> (2017).
8. Kim, M. *et al.* Lensless and optical physically unclonable function with fibrous media. *2021 Conf. on Lasers Electro-Optics Eur. & Eur. Quantum Electron. Conf. (CLEO/Europe-EQEC)* 1–1, DOI: <https://doi.org/10.1109/CLEO-Europe-EQEC52157.2021.9541599> (2021).
9. Mesaritakis, C. *et al.* Physical unclonable function based on a multi-mode optical waveguide. *Sci. Reports* **8**, DOI: <https://doi.org/10.1038/s41598-018-28008-6> (2018).
10. Masataka, N. Rayleigh backscattering theory for single-mode optical fibers. *J. Opt. Soc. Am.* **73**, 1175–1180, DOI: <https://doi.org/10.1364/JOSA.73.001175> (1983).
11. Froggatt, M. E., Soller, B. J., Gifford, D. K. & Wolfe, M. S. Correlation and keying of rayleigh scatter for loss and temperature sensing in parallel optical networks. *Opt. Fiber Commun. Conf. 2004. OFC 2004* **2**, 3 pp. vol.2– (2004).
12. Froggatt, M. E. & Gifford, D. K. Rayleigh backscattering signatures of optical fibers—their properties and applications. *Opt. Fiber Commun. Conf. Fiber Opt. Eng. Conf. 2013* **2**, OW1K.6, DOI: <https://doi.org/10.1364/OFC.2013.OW1K.6> (2013).
13. Gifford, D. K. & Froggatt, M. E. Rayleigh scatter based high resolution distributed fiber sensing for safety and security applications. *Front. Opt. 2013 FW4I.2*, DOI: <https://doi.org/10.1364/FIO.2013.FW4I.2> (2013).
14. Du, Y., Jothibasu, S., Zhuang, Y., Zhu, C. & Huang, J. Unclonable optical fiber identification based on rayleigh backscattering signatures. *J. Light. Technol.* **35**, 4634–4640, DOI: <https://doi.org/10.1109/JLT.2017.2754285> (2017).
15. MacDonald, R. I. Frequency domain optical reflectometer. *Appl. Opt.* **20**, 1840–1844, DOI: <https://doi.org/10.1364/AO.20.001840> (1981).
16. Barnoski, M. K., Rourke, M. D., Jensen, S. M. & Melville, R. T. Optical time domain reflectometer. *Appl. Opt.* **16**, 2375–2379, DOI: <https://doi.org/10.1364/AO.16.002375> (1977).
17. Brinkmeyer, E. Analysis of the backscattering method for single-mode optical fibers. *J. Opt. Soc. Am.* **70**, 1010–1012, DOI: <https://doi.org/10.1364/JOSA.70.001010> (1980).
18. Hartog, A. & Gold, M. On the theory of backscattering in single-mode optical fibers. *J. Light. Technol.* **2**, 76–82, DOI: <https://doi.org/10.1109/JLT.1984.1073598> (1984).
19. Alekseev, A. E., Tezadov, Y. A. & Potapov, V. T. The influence of the degree of coherence of a semiconductor laser on the statistic of the backscattered intensity in a single-mode optical fiber. *J. Commun. Technol. Electron.* **56**, 1490–1498, DOI: <https://doi.org/10.1134/S10642269112014X> (2011).

Acknowledgements

We thank our colleague Nikita Kirsanov for the useful discussions.

Author contributions statement

M.J. and A.S. conducted the experiments. E.Z., M.J. and A.S. wrote the initial manuscript. M.V. supervised the project. All authors analyzed the data and contributed to the final manuscript.

Competing interests

The authors declare no competing interests.

Additional information

Correspondence and requests for materials should be addressed to M.J.

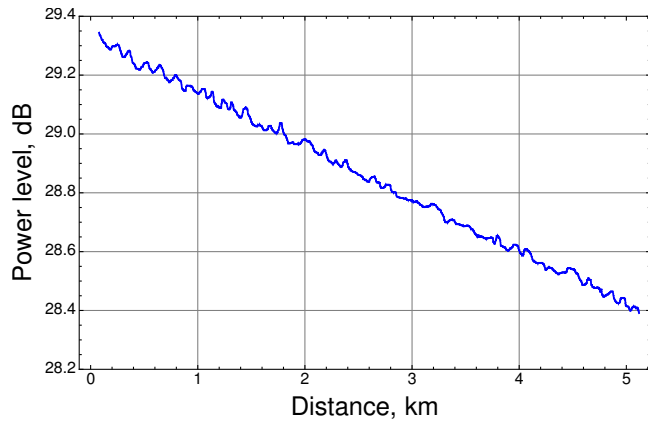


Figure 1. An example of experimentally obtained reflectogram of a homogeneous section of optical fiber. Deviations from the linear trend are mainly due to inhomogeneities in the optical fiber. The measurements were carried out for a standard single-mode fiber SMF-28e (ITU-T G.652.D) at a wavelength of $\lambda=1550$ nm with a pulse duration of 500 ns and averaging over 2^{10} .

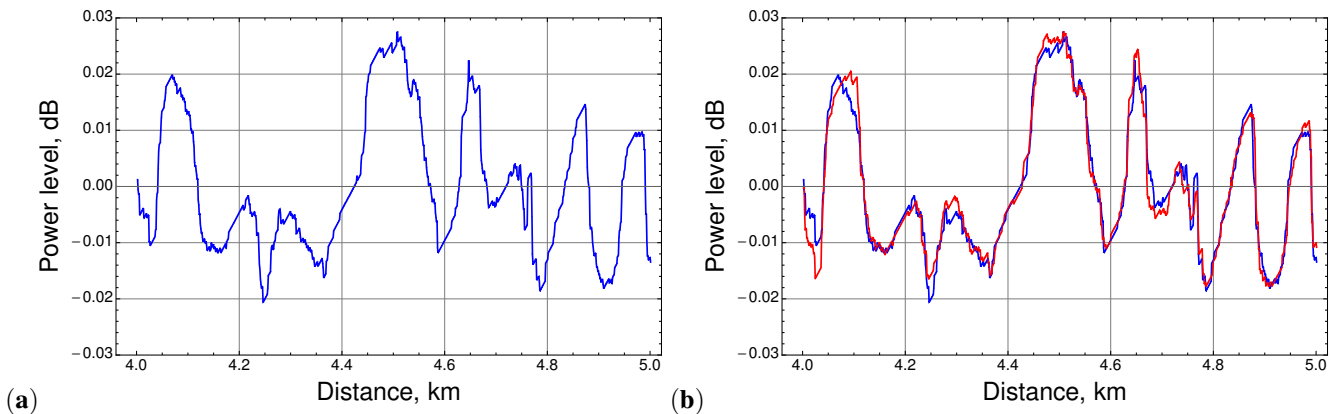


Figure 2. (a) An example of unique patterns remained after subtracting the linear contribution from the reflectogram. The measurements were carried out for a section of a standard single-mode fiber SMF-28e (ITU-T G.652.D) 1 km long at a wavelength of $\lambda=1550$ nm with a pulse duration of 500 ns and averaging over 2^{10} sampels. (b) An example of high-precision reproducibility of patterns obtained from two consecutive measurements. The red curve corresponds to a measurement taken about 10 seconds after the measurement, which corresponds to the blue curve. Both measurements were carried out with pulse parameters the same as in (a) and with the same fiber section as in (a).

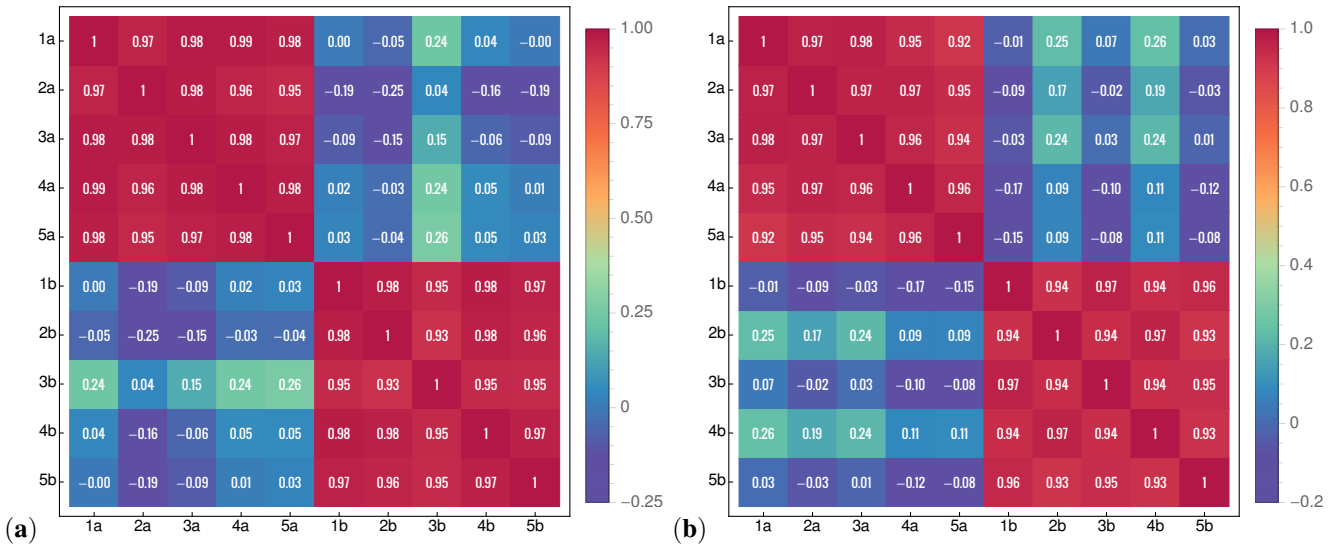


Figure 3. Experimental confirmation of uniqueness of fiber keys. (a) Joint correlation matrix for two series of 5 measurements of two sections of a standard SMF-28e (ITU-T G.652.D) single-mode fiber, each 100 m long. The nearest section is 20 km away from the reflectometer. The measurements were carried out at a wavelength of $\lambda=1550$ nm with a pulse duration of 500 ns and an averaging of 2^{10} . Series "a" corresponds to the first fiber section and the series "b" corresponds to the second. (b) Joint correlation matrix for two series of 5 measurements of single fiber section 100 m long, which is 20 km away from the reflectometer. The measurements were carried out at a wavelength of $\lambda=1550$ nm with 2^{10} averaging, but with different pulse durations. Series "a" corresponds to the duration of 500 ns and series "b" corresponds to the duration of 1000 ns.

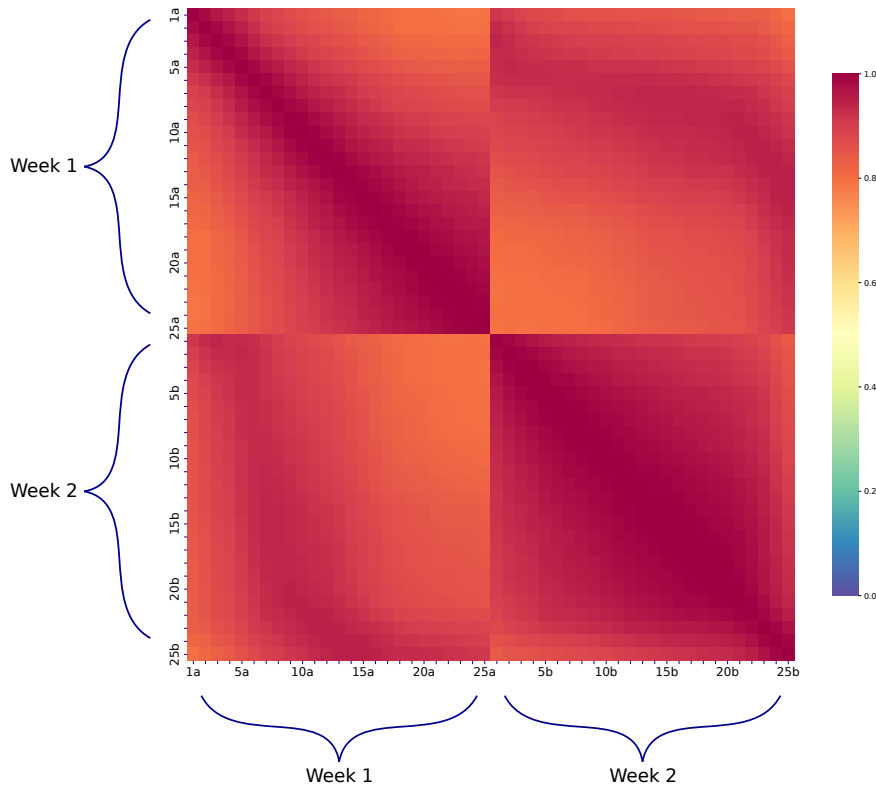


Figure 4. A joint correlation matrix for two measurement series of a section of a standard SMF-28e (ITU-T G.652.D) single-mode fiber 400 m long. The measurements were carried out at a wavelength of $\lambda = 1550$ nm with a pulse duration of 500 ns and an averaging of 2^{14} . The time difference between consecutive experiments into same series is 2 minutes. The time difference between the series is one week. Since all values of the correlation matrix are greater than 0.80, long-time reproducibility of observed patterns is established.

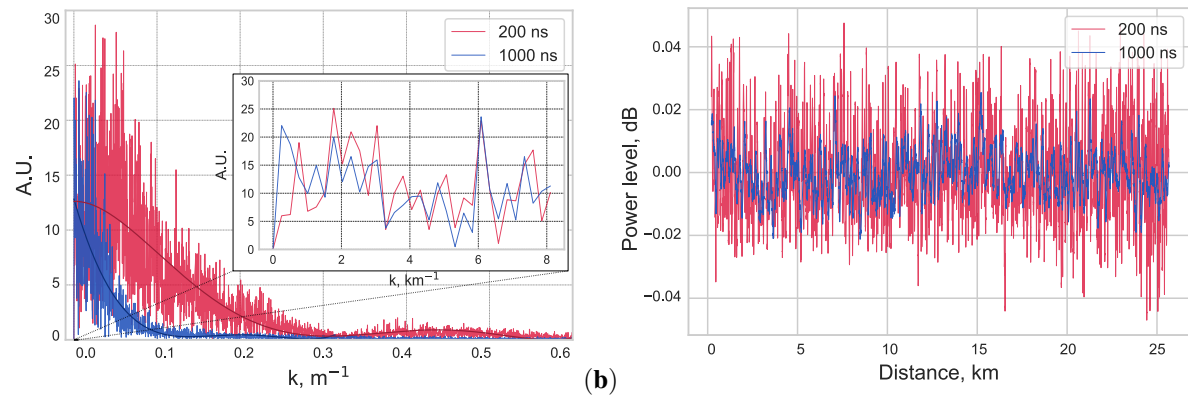


Figure 5. (a) The absolute values of discrete Fourier transform (DFT) of patterns represented in (b). Curved lines represent the polynomial approximations of data. The subplot represents the starting region of the main plot. (b) Patterns corresponding to 25 km long fiber line with a standard single-mode fiber SMF-28e (ITU-T G.652.D). The red curve corresponds to a measurement with a pulse duration of 200 ns and the blue curve corresponds to a measurement with a pulse duration of 1000 ns. Both measurements were carried out at a wavelength of $\lambda=1550$ nm with 2^{10} averaging.

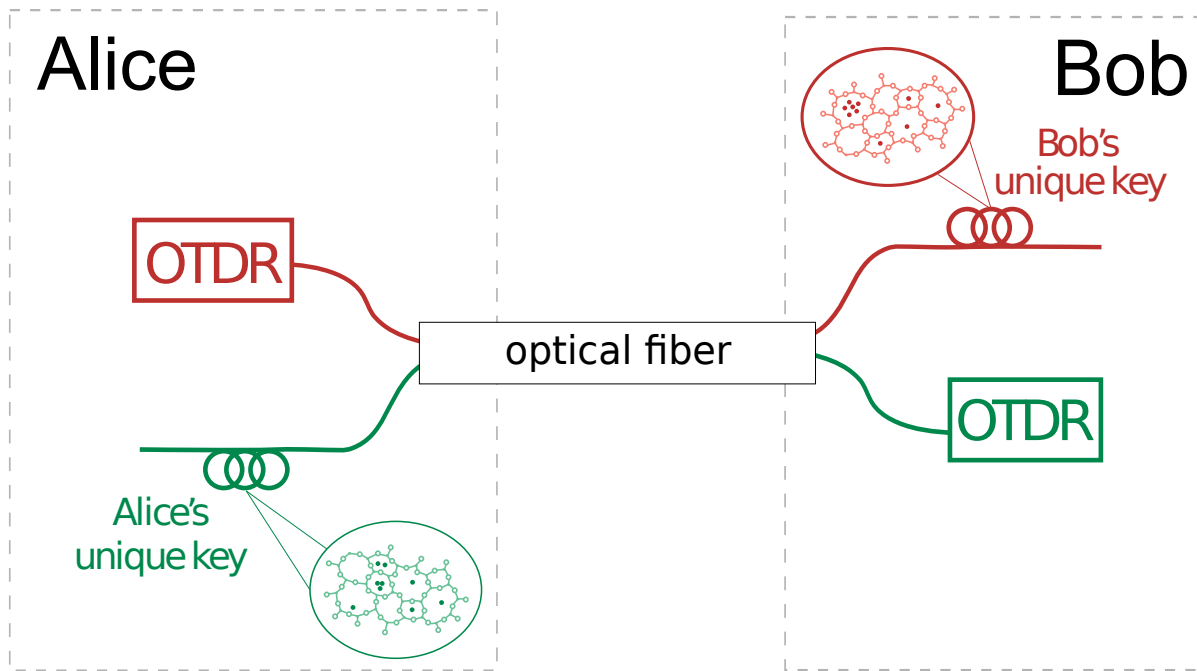


Figure 6. Authentication scheme for the legitimate users and the fiber line. Bob authenticates Alice (the green configuration) or Alice authenticates Bob (the red configuration). The authenticated user connects his own unique section of fiber to his end of the line. The obtained reflectogram of corresponding section will be considered as unique response which determines the authentication success. Moreover, each user can additionally authenticate any section of the fiber line at will.